



## Experimental Study of Properties of Green Concrete Based on Geopolymer Materials under High Temperature

Mansourghanaei, M.H.<sup>1\*</sup>, Biklaryan, M.<sup>2</sup> and Mardookhpour, A.<sup>3</sup>

<sup>1</sup> Ph.D., Department of Civil Engineering, Chalous Branch, Islamic Azad University, Chalous, Iran.

<sup>2</sup> Assistant Professor, Department of Civil Engineering, Chalous Branch, Islamic Azad University, Chalous, Iran.

<sup>3</sup> Assistant Professor, Department of Civil Engineering, Lahijan Branch, Islamic Azad University, Lahijan, Iran.

© University of Tehran 2022

Received: 04 Jul. 2022;

Revised: 12 Sep 2022;

Accepted: 08 Oct. 2022

**ABSTRACT:** Geopolymer Concrete (GPC) are known as green and nature-friendly concretes. In the current research, GPC based on Granulated Blast Furnace Slag (GBFS) was used with 0-2% Polyolefin Fibers (POFs) and 0-8% Nano Silica (NS) to improve its structure. After curing the specimens under dry conditions at a temperature of 60 °C in an oven, then subjected to permeability test, water absorption test and Ultrasonic Pulse Velocity (UPV) test at the ages of 7, 28 and 90 days. On the other hand, NS reduced the amount of water absorption and water permeability in concrete by 24 and 44%, this is due to the property of filling the pores with NS. Moreover, by conducting the ultrasonic, X-Ray Fluorescence (XRF), X-Ray Diffraction (XRD), and Scanning Electron Microscope (SEM) tests, a microstructure investigation was carried out on the concrete samples. In addition to their overlapping with each other, the results indicate the GPC superiority over the regular concrete. Besides, it demonstrated the positive influence of NS addition on the UPV and microstructural properties concretes against the heating treatment at the age of 90 days. Heat caused a drop in the results by destroying the concrete microstructure.

**Keywords:** Concrete Microstructure, Geopolymer Concrete, Granulated Blast Furnace Slag, Nano Silica, Polyolefin Fibers.

### 1. Introduction

Geopolymers are newly emerging adhesive materials that are able to replace ordinary Portland cement (OPC), while producing less toxic gas CO<sub>2</sub> and consuming less energy in the production process. (Ahmed et al., 2022). For this reason, this type of concrete is known as green and nature-friendly concrete. Geopolymers are

materials with cement properties that are comparable to OPC due to environmental benefits (Lyu et al., 2022). GPC is one of the innovative eco-friendly materials that has gained the attention of many researchers in the sustainable development of the construction industry (Sathish Kumar et al., 2022). GPC are known as a suitable alternative to Ordinary Portland Cement Concrete (OPCC) due to their superior

\* Corresponding author E-mail: [mhm.ghanaei@iauc.ac.ir](mailto:mhm.ghanaei@iauc.ac.ir)

mechanical properties and durability. (Verma and Dev, 2022). Green concrete based on GPC has many environmental advantages. So that, geopolymer concretes have lower CO<sub>2</sub> emissions than conventional concrete and Portland cement (Asadi et al., 2022; Memiş et al., 2022; Jindal et al., 2022; Kanagaraj et al., 2022; Erfanimanesh and Sharbatdar, 2020). Research shows that in order to reduce toxic gas CO<sub>2</sub> up to 55%, it is necessary to use sustainable materials such as GPC (Asadi et al., 2022). In the last three decades, the gigantic demand for sustainable and environmentally friendly concrete with reduced environmental footprints has resulted in the development of low carbon concretes such as GPC (Jindal et al., 2022). GPC is economical, stable, environmentally friendly and durable concrete (Verma et al., 2022). GPC is produced under the process of geopolymerization, in which a molecular network is formed with Coulancy bonds (Wong, 2022). GPC has superior mechanical properties and durability compared to conventional concrete (Srividya et al., 2022). In GPC, GBFS were used as binder material, along with sodium hydroxide and sodium silicate solutions as activator solutions (Kanagaraj et al., 2022). Geopolymer adhesive materials are recognized as a potential and sustainable alternative to conventional concrete (Albidah et al., 2022). Increasing the concentration of the molarity of active alkali solution in the composition of GPC leads to the improvement of the properties of GPC to a certain extent (Shilar et al., 2022). SEM images of the microstructure of GPC show the superiority of this type of concrete compared to ordinary concrete (Amin et al., 2022).

Recently, many efforts have been made to use nanoparticles such as NS in GPC to improve the properties of this type of concrete (Ahmed et al., 2022). These nanoparticles improve the properties of concrete by increasing the speed of the geopolymerization process (Shilar et al., 2022). Nanoparticles, by producing a large

volume of hydrated gels such as C-S-H, N-A-S-H and C-A-S-H by filling holes and pores, improve durability and strength in hardened concrete (Ahmed et al., 2022). Several factors such as the proportion of active alkali solution, age of concrete curing and heat curing temperature in concrete are effective on the quality of GPC containing NS (Ahmed et al., 2022). In addition, the presence of NS particles in the composition of GPC leads to the acceleration of the geopolymerization process (Assaedi et al., 2019).

According to the studies, using macro plastic fibers for concrete improvement instead of metal mesh and fibers has captured researchers' attention (Abbasi Nattaj Omran., 2022). The concrete-related industries widely use polyolefin-based fibers (Alberti et al., 2015). By bridging the cracks in the hardened concrete mix, POF prevent the development of cracks against the incoming loads (Yousefvand., 2019). By performing Crack Mouth Opening Displacement (CMOD) analysis, POFs with proper connection in the concrete composition and due to the high strength of these fibers lead to the improvement of concrete properties (Adhikary, 2019).

Although the use of GPC as one of the emerging building materials is expanding, but the resistance of this type of concrete against high heat in the long term needs to be known more (Amran et al., 2022). In this regard, research has shown that geopolymers, in addition to environmental properties, have good resistance to high temperatures (Albidah et al., 2022).

The properties and the bonding type are different in regular and GPCs. The bonding in regular concretes is based on calcium oxide hydration and silicon dioxide reactions in order to form calcium silicate hydrate. However, the GPC bonding is established via alkaline activator contact with the Aluminosilicate raw materials, reshaped in the polymerization reaction product, and slowly cooled in a high pH medium and hydrothermal condition (hydrothermal condition is referred to the

chemical reactions in the presence of solvent in higher pressure and temperature). This structure (related to the GPC) has some merits compared to the regular concrete, e.g. it provides better resistance performance at higher temperatures (Aslani, 2016).

A higher temperature brings about physical and chemical changes in the concrete structure, accompanied by resistance performance decline and concrete destruction. Although concrete is one of the insulating building materials against heat, if it is exposed to a higher temperature, irreversible physical and chemical changes will take place. Some damages created as a result of concrete placement against the heat exposure are indicated as follows. Resistance performance decline, weight loss, and the formation of large cracks and cavities in the micro and macrostructure of concrete.

- The removal of evaporative water at 100 °C.
- Calcium Silicate Hydrates hydration starts at 180 °C; as the temperature increases to 200 °C, the vapor pressure continuously elevates in the geopolymer structure.
- The OH hydroxyl groups are evaporated at 500 °C. The dihydroxylation changes the Aluminosilicate structure, reducing the resistance level.
- An intensely porous ceramic structure is formed at 800 °C.

The changes occurring at a temperature higher than 500 °C in concrete are irreversible, and the changes made in the concrete behavior are more obvious at such temperatures. Some researchers have reported that reduction in resistance is mainly attributed to the breakdown of calcium hydroxide, and this phenomenon usually takes place in the temperature range between 450 to 500 °C (Bentz et al., 2000).

This study mainly aims to investigate the durability and microstructural properties of the GPCs based on the GBFS containing NS and also reinforced with POFs. In this way, while producing green concrete based on

GPC, concrete with superior advantages over OPCC can be produced. For this purpose, the water absorption and water permeability tests under room temperature and UPV, SEM, XRD and XRF tests under room temperature and high heat have been conducted.

## 2. Experimental Program and Test Methods

### 2.1. Materials

In this experimental study, according to other articles (Mansourghanaei et al., 2022), the Portland cement type II with a 2.35 g/cm<sup>3</sup> of specific weight according to standard En 197-1 and the GBFS was with the density of 2.79 g/cm<sup>3</sup> according to ASTM C989/C989M standard. The chemical properties of these materials are indicated in Table 1. The used fine aggregates with a density of 2.75 g/cm<sup>3</sup>, and the coarse aggregates with a maximum size of 19 mm and a density of 2.65 g/cm<sup>3</sup> according to ASTM-C33. The curing was performed at a temperature of 60 °C. NS was used with a purity of 99.9% and a particle size of 15-25 nm. POFs were used in a wavy form with a length of 30 mm under the standard ASTM D7508/D7508M, whose physical properties are shown in Table 2.

**Table 1.** Chemical compositions of materials

Component	GBFS (%)	Portland cement type II (%)
SiO <sub>2</sub> (%)	29.2	21.3
Al <sub>2</sub> O <sub>3</sub> (%)	19.4	4.7
Fe <sub>2</sub> O <sub>3</sub> (%)	5.8	4.3
CaO (%)	38.6	62.7
MgO (%)	2.8	2.1
SO <sub>3</sub> (%)	2.6	2
K <sub>2</sub> O (%)	0.1	0.65
Na <sub>2</sub> O (%)	0.2	0.18
TiO <sub>2</sub> (%)	0.6	-
Free Cao Blaine (cm <sup>2</sup> /gr)	-	1.12
	2200	3200
LOI (%)	0.3	1.84

**Table 2.** Physical properties of the POFs

Tensile Strength (N/mm <sup>2</sup> )	> 500
Length (mm)	30
Diameter (mm)	0.8
Elasticity Modulus (GPa)	>11
Bulk Density (Kg/m <sup>3</sup> )	2400

## 2.2. Mix Design

According to other articles (Mansourghanaei et al., 2022), GPC under the standard is made in 6 mixing designs, the first design is made of ordinary concrete and the 2<sup>nd</sup> to 5<sup>th</sup> designs are made of geopolymeric concrete based on the slag of the slag containing different percentages of NS and polyolefin fibers. A 12 M active alkali solution of NaOH and Na<sub>2</sub>SiO<sub>3</sub> was used. Table 3 lists the mix designs of the specimens.

## 2.3. Test Methods

After fabricating the samples, for better curing and increasing the durability and microstructural properties, the samples were at 80 °C with a thermal rate of 4.4 °C/min for 48 h. After curing the samples and before performing the tests, the samples were placed in an oven at 500 °C for 1 h at the age of 90 days. In the end, by opening the oven door, the samples reached the ambient temperature (Wong, 2022). Then, the necessary tests were performed on concrete samples according to the relevant standards at ambient temperature and under high temperature.

The water absorption test was carried out according to the standard ASTM C1585-04 and at first the concrete samples were dried under 50±5 °C temperature for three days. Then, after cooling, the samples were kept at room temperature for 15 days. A plastic cover was used to prevent water evaporation (Albitar et al., 2017). The water absorption coefficient was calculated based on the following equation (De Beer et al., 2005):

$$S = \frac{(Q/A)}{\sqrt{t}} \quad \left(\frac{m}{\sqrt{t}}\right) \quad (1)$$

where  $Q$ : is volume of the absorbed water,  $A$ : is area of the concrete in contact with water, and  $t$ : is time.

The water permeability test under the EN 12390-8 standard was performed on 15 cm cubic samples, in which the concrete samples were subjected to water pressure

50±500 kPa for 72 hours. The water penetration coefficient was calculated according to Eq. (2) (Ahmad et al., 2017):

$$K = \frac{e^2 v}{2ht} (m/s) \quad (2)$$

where  $e$ : is penetration depth (m),  $v$ : is volume fraction of concrete,  $h$ : is hydraulic length of concrete, and  $t$ : is the duration it is under water pressure.

The UPV tests (Galan, 1967) were conducted according to ASTM C597 using a non-destructive ultrasonic electronic apparatus, PUNDIT MODEL PC1012, with an accuracy of ±0.1 μs for a transformer with a vibrational frequency of 55 kHz and a movement time accuracy of ±2% for the distance.

## 3. Results and Discussion

### 3.1. The Results of The Water Absorption Test

The results of the water absorption test in concrete are shown in Figure 1. Increasing the curing age in concrete has led to a decrease in water penetration in concrete. In this regard, the age of 28 days compared to the age of 7 days has experienced the superiority of the results between 11-32% and the age of 90 days compared to the age of 28 days has experienced the improvement of the results of 2-18%. At the age of 90 days, GPC has 40% less water absorption than normal concrete. Adding silica nanoparticles to the GPC mix up to 24% and adding POFs to the GPC mix up to 24% improved the results.

### 3.2. The Results of The Water Permeability Test

The results of the water permeability test in concrete are shown in Figure 2. Based on these results, normal concrete is in the poor classification and GPC is in the average classification of concrete quality (Rendell et al., 2010). The results of this section indicate that GPC has 16% less water permeability than normal concrete. The

addition of NS particles to the composition of geopolymeric concrete has improved the results of water permeability in this type of concrete by 44%. On the other hand, adding up to 2% of POFs in the composition of geopolymeric concrete has led to an improvement of the results by 55% (compared to samples of geopolymeric concrete without fibers). The permeability of water in concrete has a direct relationship

with the amount of porosity in the concrete composition, so that with the increase of porosity in concrete, the penetration of water in concrete increases.

Figure 3 shows the concrete sample measuring the amount of water penetration in the concrete. The relationship between the capillary water absorption coefficient and the water permeability coefficient in concrete is shown in Figure 4.

**Table 3.** Details of the mix designs

Mix No.	Mix ID	OPC (Kg/m <sup>3</sup> )	GBFS (Kg/m <sup>3</sup> )	Water (Kg/m <sup>3</sup> )	Alkaline solution	NS (Kg/m <sup>3</sup> )	NS (%)	Coarse aggregates (Kg/m <sup>3</sup> )	Fine aggregates (Kg/m <sup>3</sup> )	POFs (Kg/m <sup>3</sup> )	POFs (%)	Super plasticizer (Kg/m <sup>3</sup> )
1	OPCC	450	0	202.5	0	0	0	1000	761	0	0	9
2	GPCNS0P00	0	450	0	202.5	0	0	1000	816	0	0	9
3	GPCNS4P00	0	432	0	202.5	18	4	1000	767	0	0	10
4	GPCNS8P00	0	414	0	202.5	36	8	1000	718	0	0	11
5	GPCNS8P01	0	432	0	202.5	36	8	1000	672	24	1	11
6	GPCNS8P02	0	432	0	202.5	36	8	1000	646	48	2	11

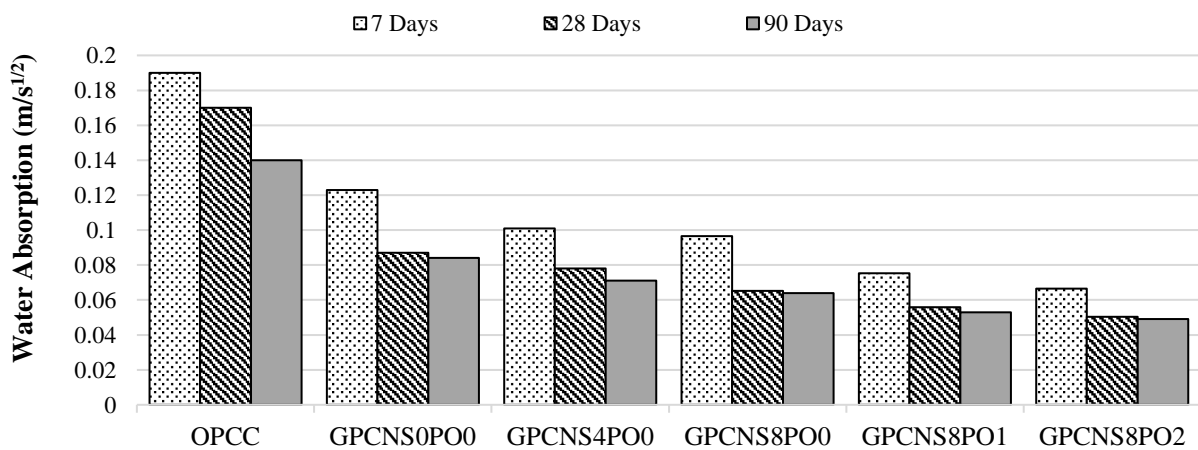


**Fig. 1.** Water absorption variations in specimens

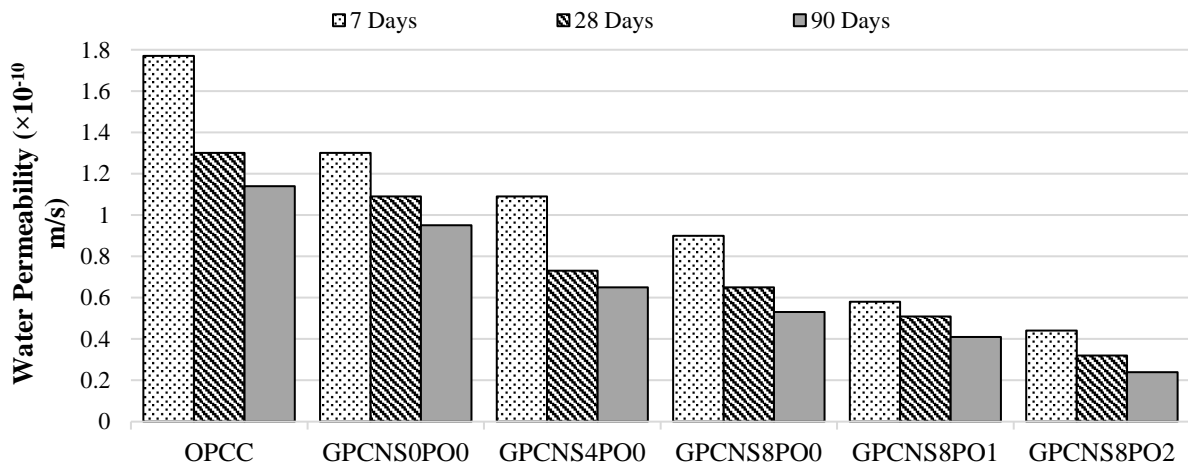


**Fig. 2.** Variations in the permeability coefficients of the specimens



Fig. 3. The amount of water permeability in the specimens

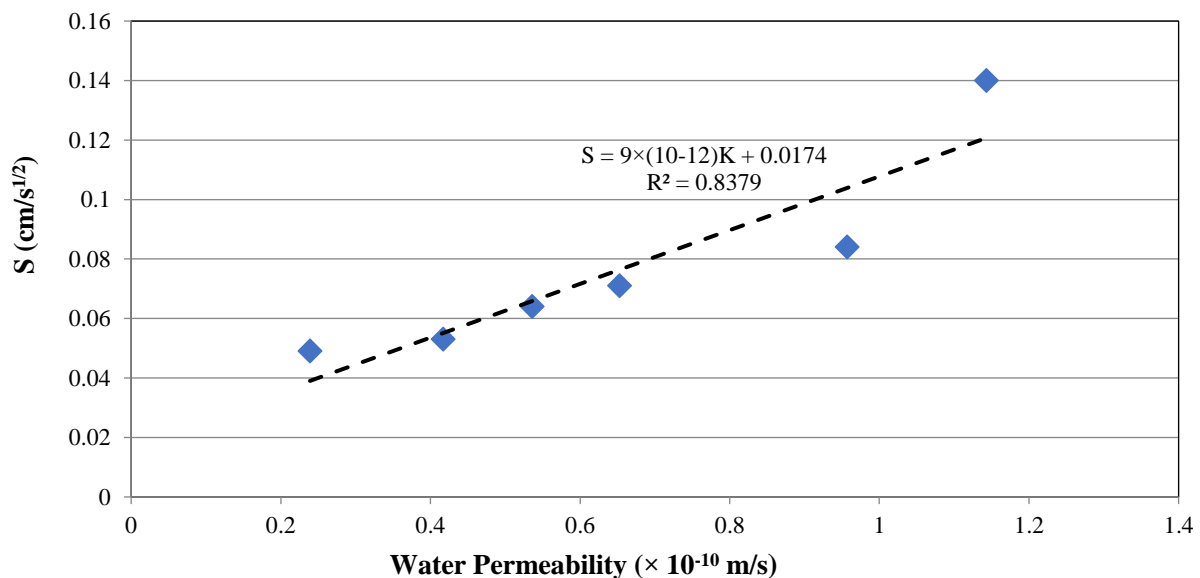


Fig. 4. The relationship between permeability and water absorption

### 3.3. The Results of The Ultrasonic Pulse Velocity (UPV) Test

The velocity of the ultrasonic waves passing through the samples can be seen at ambient temperature (7,28,90 days) in Figure 5 and under heat (90 days) in Figure 6. The speed quality of ultrasonic waves based on IS 13311-1 standard in four levels as follows: Doubtful with a speed below 3000 m/s, Moderate with a speed of 3000 to 3500 m/s, Good with a speed of 3500 to 4500 m/s and Excellent with a speed of more than 4500 m/s is divided.

The results obtained in this section indicate a decline in transient ultrasonic wave velocity after putting concrete samples under heating treatment such that transition velocity of ultrasonic waves decreased by 37% and 46% in regular

concrete and GPC at 500 °C, respectively. By the addition of 4% and 8% NS to the GPC compound, the transition velocity of ultrasonic pulse declined by 40% and 37%, respectively. The results indicated that the addition of fibers reduced the UPV. This reduction was not significant being in the range lower than 12.5%. The small effect of fibers on the pulse velocity was also reported, this rise can be originated from the fact that the pulse velocity in steel is 1.2-1.9 times more than that in GPC (Reufi et al., 2016). According to the obtained results in this investigation, all designs at room temperature have "superior" quality, and all samples at 500 °C have average and good quality (Whitehurst, 1951). As long as the UPV values are classified as "excellent", the concrete has no large cracks or pores that

can affect the integrity of the specimen structure (Kwan et al., 2012). On the other hand, the obtained results revealed that the addition of NS increased the pulse velocity by filling the pores and densifying and integrating the concrete. Due to the curing in the dry environment of the oven, some fine cracks and pores were formed in the GPC preventing its full integrity, which allows for the transmission of ultrasonic

pulses with higher velocities. Therefore, the obtained velocities were slightly lower than those of OPCC. Nevertheless, these cracks had very fine dimensions and could only influence the UPV having no remarkable effect on the compressive strength of the specimens (Ren et al., 2016). The presence of NS in mix design GPCNS8PO0 was very effective in making the velocity of the passing pulses close to those of the OPCC.

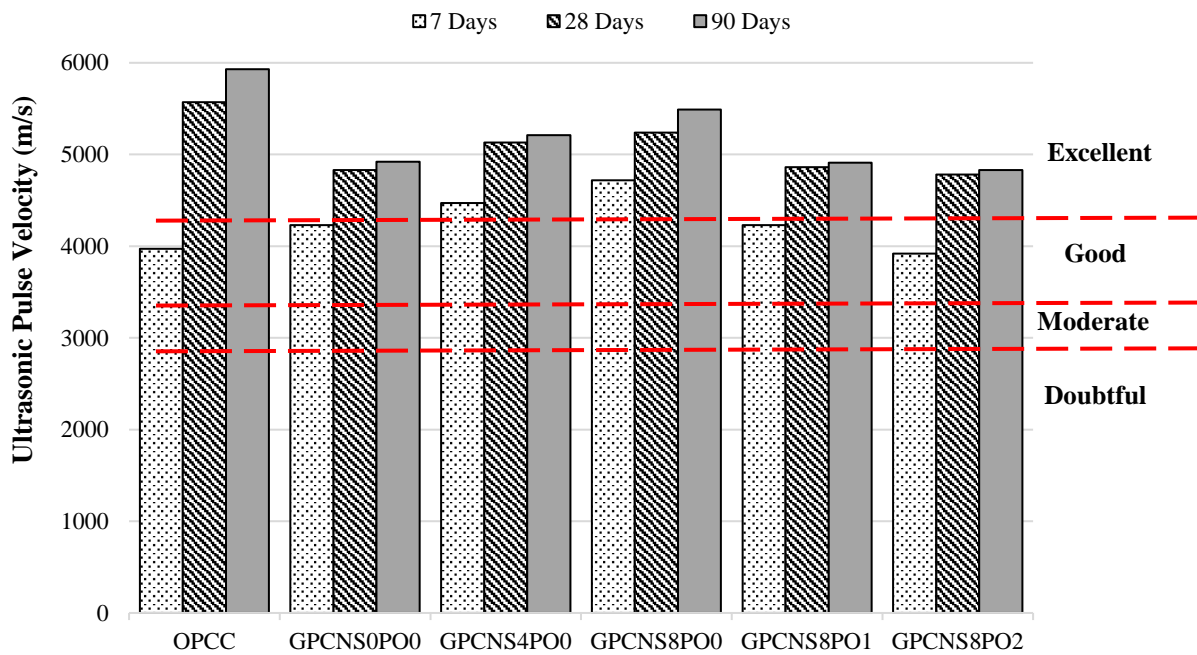


Fig. 5. The variations in the ultrasonic pulse velocities of the specimens

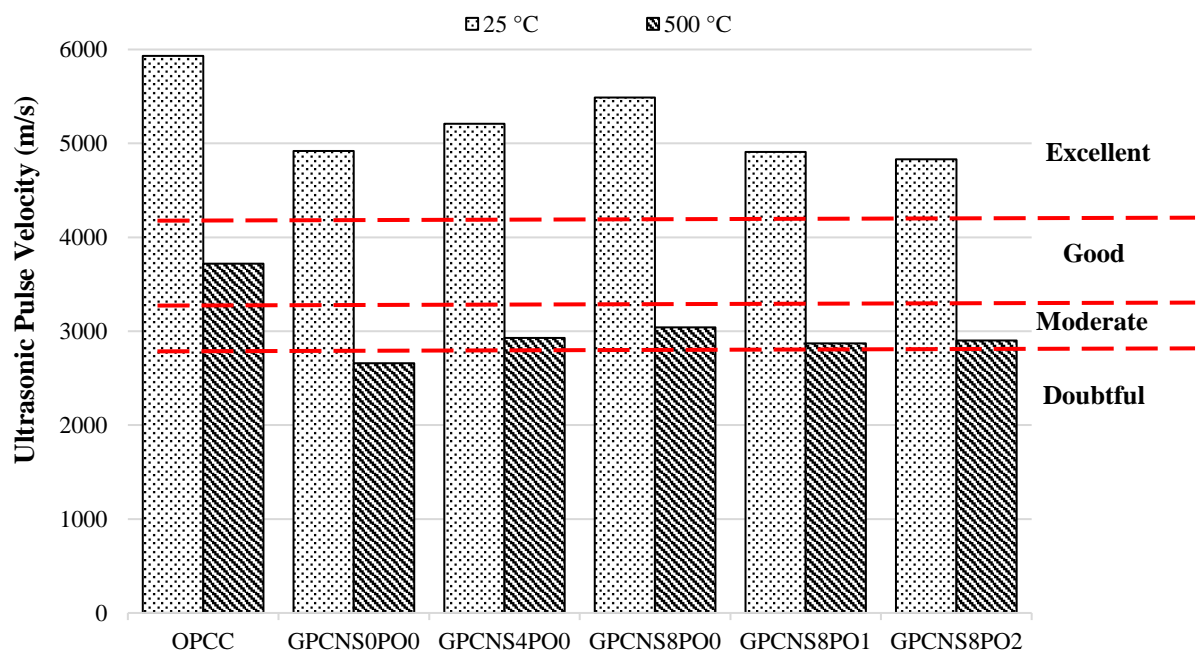


Fig. 6. The variation in ultrasonic wave velocity of samples

#### 4. The Results of the SEM, XRD and XRF Tests

Figure 7 demonstrates microscopic images of regular concrete containing Portland cement at different temperatures. Figure 8 indicates microscopic images of GPC based on GBFS at different temperatures. The chemical reaction process in GPC is more than normal concrete (Du et al., 2014). Due to the porous structure of geopolymer and micro pores at micro and nano scales, GPC allows water evaporation without damaging the Aluminosilicate network, leading to the greater durability of geopolymers than regular concrete high temperatures. Various chemical compounds can be seen in the Figure 9. Microcracks, cavities, amorphous structure of Aluminosilicate, and ceramic structure in GPC can be seen. Compact and homogenous Aluminosilicate structure in geopolymer sample at room temperature, which is the results of geopolymerization process, is indicated. GBFS is full of calcium. In geopolymeric concrete based on blast furnace slag, geopolymerization products include hydrated gels such as C-S-H, A-S-H, C-A-S-H and N-A-S-H. These gels are the main factor of strength in hardened geopolymer paste. On the other hand, these gels improve durability in concrete. With the passage of time, the geopolymerization process and the volume production of hydrated gels develop in the concrete composition (Mansourghanaei et al., 2022).

As can be seen in Figure 8 for geopolymer samples at 500 °C, OH of hydroxyl groups dehydrate at this temperature, and OH is located on the surface and edges of each geopolymer micelle. The dehydroxylation process affects and declines durability properties. As the dehydroxylation process begins, the structure of Aluminosilicate is changing to calcium carbonate and appears in the form of crystal and semi-crystal structures. As crystal structures increases, microcracks and cavities expand. An increase in temperature leads to the formation and

destruction of new carbonate minerals. On the other hand, as crystal structures decrease, cavities and cracks increase on geopolymer structure. Dehydration takes place between 100 °C and 300 °C, and Dehydroxylation takes place between 500 °C and 900 °C. On the other hand, heat destroys C-A-S-H and C-S-H microstructures in GPC. Applying a great deal of heat converts amorphous geopolymer Aluminosilicate to a ceramic-like structure.

At a temperature higher than 100 °C, the sample shrinks, and cracks appear since water leaves geopolymer structures and the hydration process begins. According to studies conducted by other researchers, when vapor pressure reaches its maximum value, the compact structure of geopolymer with low permeability will not be able to control thermal stresses. This will lead to the creation of thermal cracks on the sample surface due to shrinkage. This phenomenon is known as the "vapor effect" (Hu et al., 2009). Besides, water evaporation from the geopolymer structure is accompanied by weight reduction, leading to the creation of thermal cracks due to shrinkage.

At a temperature condition of 500 °C, geopolymer microstructures change and become destroyed, leading to crystal structure formation. In addition, at high temperatures, superficial and internal cracks are created on the geopolymer structure. It is attributed to calcite decomposition and carbon dioxide release. Carbon dioxide release creates cracks on samples. High expansion and extended cracks change the size and shape of samples. According to SEM images, the formation of extremely porous ceramic structures, water evaporation, and the dehydroxylation process are the main reasons behind the destruction of physical structures. Another reason behind the reduction in resistance of GPC at high temperatures can be attributed to the fact that the presence of strong alkaline activator in GPC under laboratory conditions produces a matrix of highly reactive

Aluminosilicate gels, while a great number of unreacted silicate forms, which undergoes densification and swelling processes at the temperature range of 500 to 800 °C.

Even though fibers change the pathway of cracks or prevent them from developing, the lack of chemical composition between fibers and materials in GPC reduces

durability. Fibers completely burn at 500 °C, and their empty spaces become pores and cavities. On the one hand, this phenomenon reduces durability features. On the other hand, these pores and cavities create a way for gases and water vapor formed inside concrete to leave it and prevent spalling and disintegration of concrete at high temperatures.

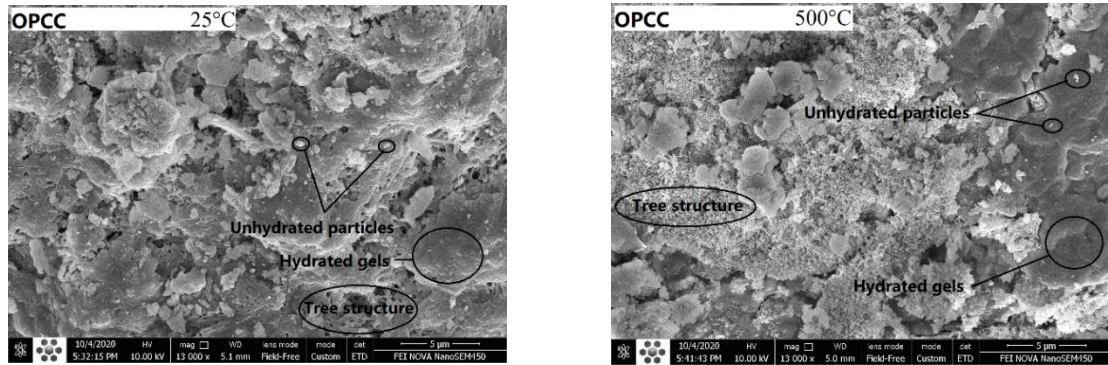


Fig. 7. SEM for the OPCC at different temperatures

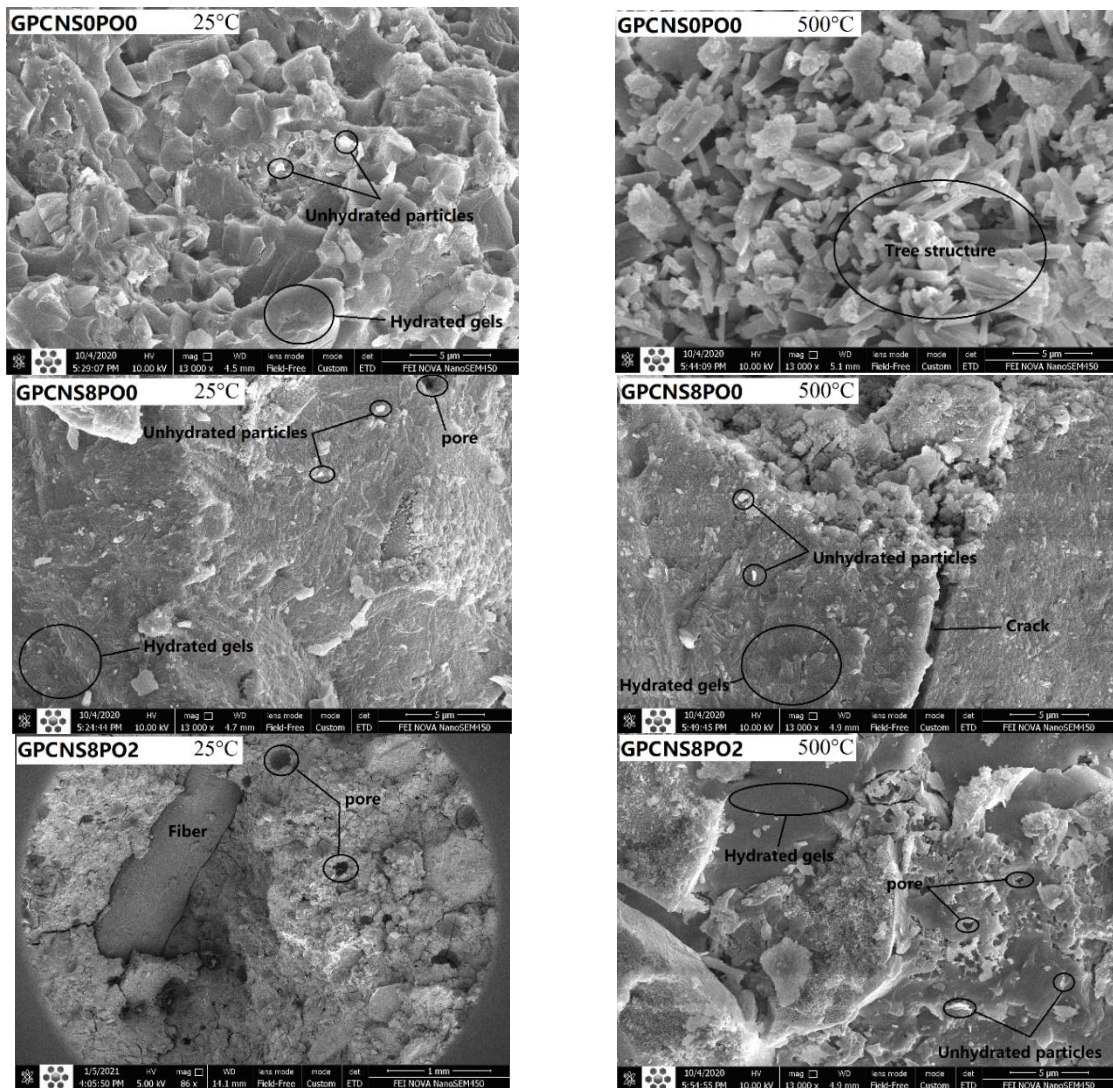


Fig. 8. SEM for the GPC at different temperatures

The results of spectrometry are shown in Figure 9, which illustrates the regular concrete XRD graph at 25 and 500 °C. At 25 °C, the crystal and quasicrystal phases of Aluminum Phosphate, Calcium Hydroxide, Titanium Oxide, Calcite, and Dolomite were observed. Besides, at 500 °C, Magnesium Calcium Carbonate, Carbon, Potassium Iron Magnesium Aluminum Silicate, and Calcium Aluminium Silicate Hydrate were observed.

At a higher temperature, CH gel does not turn into Calcium Carbonates, e.g. Calcite. As indicated in the graph, the CH disappears at a higher temperature, turning into Carbon and C-A, the main reason behind concrete's weakness at a high temperature (Rashad and Zeedan, 2012; Morsy et al., 2012). In the range of 29, 27, 25, and 60 angles, a number of peaks with 2200, 2000, 3000, and 3000  $\text{cm}^{-1}$  heights are observed. After being exposed to heating treatment, a number of peaks were created at 27, 28, and 29 angles and 1250, 2800, 2300  $\text{cm}^{-1}$  heights. In part b, the XRD graph is indicated for the NS-free GPC at two 25 and 500 °C. At 25 °C, the crystal and quasicrystal phases of Magnesium Calcium Carbonate, Silicon Oxide, Cristobalite, and Sodium Aluminium Silicate were observed. In addition, at 500 °C, Magnesium Calcium Carbonate, Silicon Oxide, Sodium Aluminium Silicate, and Calcium Carbonate Silicate were observed. These findings are consistent with the other researchers' findings (Fan et al., 2018; Türkmen et al., 2016).

The XRD analysis indicates that most existing peaks at greater than 1000 in the GPC graph have taken place in a region with  $26-30 = 2\theta$  angles. However, for regular concrete, the peak region is larger, and peaks at  $15-35 = 2\theta$  and 60 angles can be observed. This issue can be due to the configuration and the difference in atomic structure among the concrete samples. Therefore, the materials type and the XRD peak phases can be identified by examining the peaks' formation angle and their relative intensity. By placing the samples under the

heating treatment, it can be seen that the volume and height of the peaks are dramatically declined, demonstrating the weakening of the concrete structure in encountering heat. The GPC peaks range is in the range of 27, 28, and 29 angles. The maximum peak value for the NS-free GPC is 1300 and 1950. By being exposed to a heating treatment, it reaches 1500, 1700, and 1300.

The XRD graph for GPC containing 8% NS is demonstrated in parts 25 and 500 °C. At 25 °C, the crystal and quasicrystal phases of Calcium Carbonate, Silicon Oxide, Pyroxene, Aluminum Phosphate, and Calcite were observed. Besides, at 500 °C, Silicon Oxide, Sodium Calcium Aluminium Carbonate Silicate were observed (Adak et al., 2017; 2014; Mustakim et al., 2021).

With the increase of NS to the composition of geopolymeric concrete, the volume of hydrated gels increases, this process leads to an improvement in the strength of hardened geopolymeric concrete (Ahmed et al., 2022). With the increase of silica nanoparticles in the composition of geopolymeric concrete, geopolymeric mortar changes from crystalline to amorphous phase (Phoo-ngernkham et al., 2014; Nazari and Sanjayan, 2015).

The peaks occur at angles 27, 28, and 29, and its value is 1800, 4500, and 2200  $\text{cm}^{-1}$  at an ambient temperature. The strong peak at 1800 to 1900  $\text{cm}^{-1}$  is known as the major fingerprint for the geopolymer matrix, occurring at angles 26 to 29 degrees (Phair and Van Deventer, 2002). Additionally, the 4500 peak took place at angle 28 due to NS addition. Due to being exposed to heating treatment, the peaks reach 2100, 1350, and 1050.

In this research, XRF spectroscopy was performed under ASTM C989 standard. According to XRF results in Tables 4 and 5, compared to mixture OPCC, the  $\text{SiO}_2$  and CaO elements are declined by 28% in mixture design GPCNS0PO0 and the  $\text{Na}_2\text{O}$  content has increased from 1.1 to 15.1%. By adding 8% of NS, the  $\text{SiO}_2$  content increases by 85%, compared to mix 2.

It is worth mentioning that by comparing the samples XRF in Tables 4 and 5 at different temperatures, it can be concluded that as the temperature increases, the CaO content declines dramatically, such that this level of decrease has been 53% in design OPCC, 31% in design GPCNS0PO0, and 0.5% in design GPCNS0PO0. Besides, the temperature rise increases the SiO<sub>2</sub> percentage, such that this enhancement

reaches 41% in design OPCC, 85% in design GPCNS0PO0, and 1% in design GPCNS8PO2. Concerning the mentioned reasons in the SEM part, the reason behind these changes is totally rational. In this case, the lower resistance loss against the heat in design four can be due to more stability of the constituents when exposed to the heating treatment.

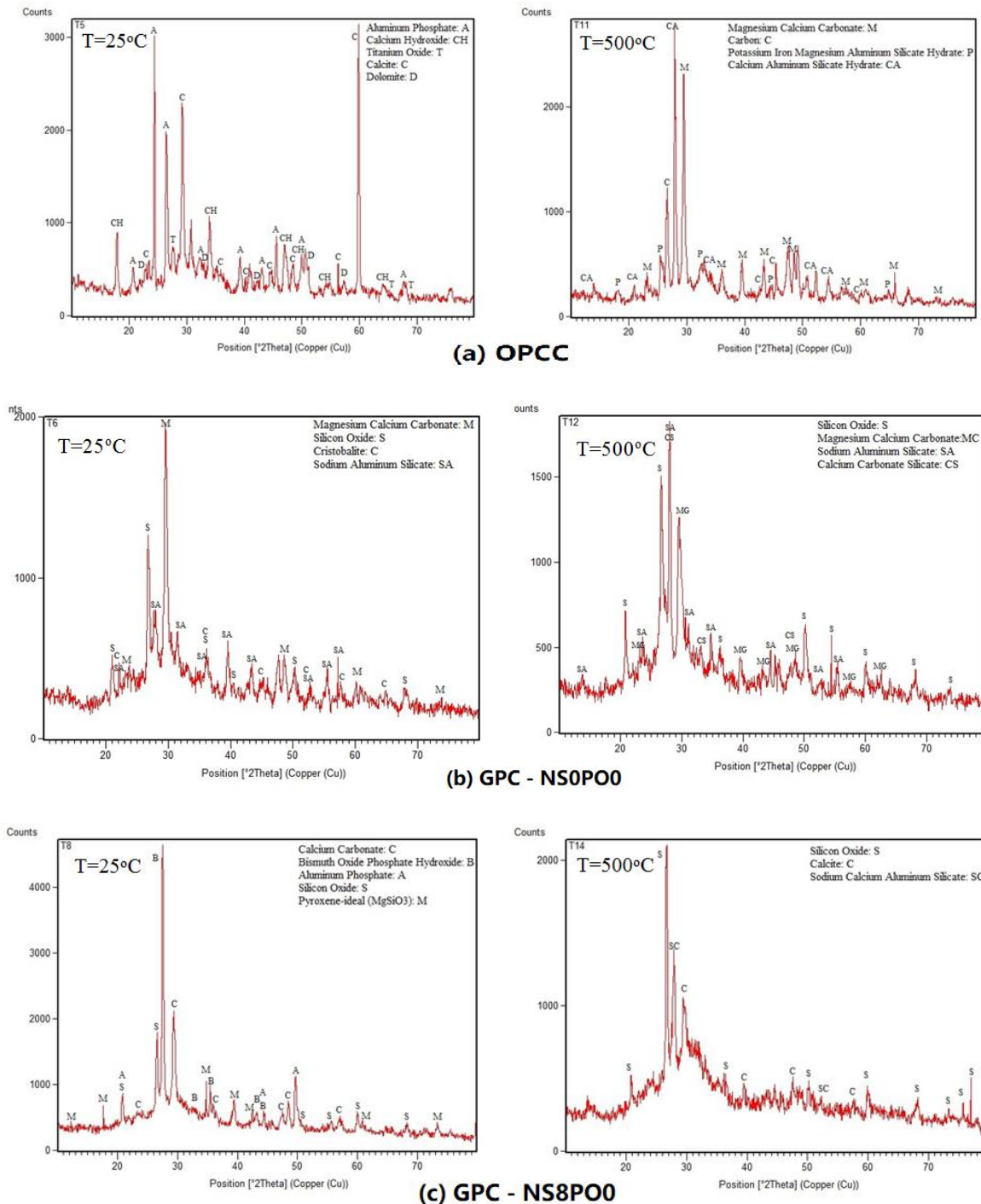


Fig. 9. XRD patterns for samples at different temperatures

**Table 4.** XRF test values for samples at ambient temperature

SO <sub>3</sub>	TiO <sub>2</sub>	LOI	Fe <sub>2</sub> O <sub>3</sub>	Na <sub>2</sub> O	K <sub>2</sub> O	MgO	CaO	AL <sub>2</sub> O <sub>3</sub>	SiO <sub>2</sub>	
1.59	0.47	16.4	7.2	1.1	0.91	2.11	37.16	5.63	27.12	<b>Mix1</b>
1.16	0.961	16.04	5.64	15.1	1.01	5.05	26.81	8.07	19.57	<b>Mix2</b>
2.8	1.17	15.7	3.94	12.87	1.05	3.01	15.2	7.01	36.33	<b>Mix4</b>

**Table 5.** XRF test values for samples at 500 °C

SO <sub>3</sub>	TiO <sub>2</sub>	LOI	Fe <sub>2</sub> O <sub>3</sub>	Na <sub>2</sub> O	K <sub>2</sub> O	MgO	CaO	AL <sub>2</sub> O <sub>3</sub>	SiO <sub>2</sub>	
2.41	0.52	16.77	9.85	1.32	1.34	1.95	17.41	9.87	38.25	<b>Mix1</b>
2.52	0.74	19.48	7.92	2.1	1.41	2.32	18.41	8.41	36.32	<b>Mix2</b>
3.54	0.87	12.95	8.24	4.87	1.5	3.14	15.12	8.21	39.87	<b>Mix4</b>

## 5. Conclusions

A major advantage of lab testing is that the samples are tested under controlled conditions (Fallah Hosseini and Hajikarimi, 2019). The addition of NS and POFs in GPC based on slag of forging furnace leads to improvement of mechanical properties and durability in this type of concrete (Mansourghanaei et al., 2022).

- In most of the tests of this laboratory research, the superiority of the properties of green concrete based on GPC compared to OPCC was obtained under ambient temperature and high temperature.
- Applying heat of 500 °C has caused fundamental changes in the microstructure of OPCC and GPC, these changes are due to evaporation of water from chemical bonding spaces in hydrated gels, which has weakened the durability properties of concrete.
- In the water permeability test in concrete, the addition of NS up to 55% and the addition of POFs up to 44% improved the results.
- Reduction of capillary water adsorption results and water permeability in fiber-containing samples can be attributed to fiber type, bonding in interfacial transfer zones and non-uniform distribution of fibers in geopolymer cement paste. Research has shown that excessive use of fibers (more than 2%) in concrete composition may lead to uneven distribution of fibers and consequently weaken the concrete structure against the forces (Connolly et al., 2014).
- The ultrasonic wave velocity determining test indicates the high quality of all

concrete samples at an ambient temperature and its higher than medium quality at 500 °C. Accordingly, NS addition increased the velocity of the waves by filling the cavities and concretes uniformity.

- The results of SEM, XRD and XRF tests well demonstrated the filling of the pores by the nanoparticles and densification of the concrete structure and bridging between the cracks by the fibers and were in coordination with the results of all tests performed in this study.

## 8. References

- Abbasi Nattaj Omrani, I., Ardeshtir-Behrestaghi, A. and Saeedian, A. (2022). "Influences of Polyvinyl Alcohol Fiber Addition on the specimen size effect and energy absorption of self-consolidating Concrete", *Civil Engineering Infrastructures Journal*, 55(1), 59-74, <https://doi.org/10.22059/cej.2021.310356.1705>.
- Adak, D., Sarkar, M. and Mandal, S. (2017). "Structural performance of nano-silica modified fly-ash based geopolymer concrete", *Construction and Building Materials*, 135, 430-439, <https://doi.org/10.1016/j.conbuildmat.2016.12.111>.
- Adhikary, S.K., Rudzionis, Z., Balakrishnan, A. and Jayakumar, V. (2019). "Investigation on the mechanical properties and post-cracking behavior of polyolefin fiber reinforced concrete", *Fibers*, 7(1), 8, <https://doi.org/10.3390/fib7010008>.
- Ahmad, S.I. and Hossain, M.A. (2017). "Water permeability characteristics of normal strength concrete made from crushed clay bricks as coarse aggregate", *Advances in Materials Science and Engineering*, 2017, 1-9, <https://doi.org/10.1155/2017/7279138>
- Ahmed, H.U., Mohammed, A.A. and Mohammed, A.S. (2022). "The role of nanomaterials in geopolymer concrete composites: A state-of-the-art review", *Journal of Building Engineering*, 49, 104062,

- <https://doi.org/10.1016/j.jobe.2022.104062>.
- Ahmed, H.U., Mohammed, A.S., Faraj, R.H., Qaidi, S.M. and Mohammed, A.A. (2022). "Compressive strength of geopolymer concrete modified with nano-silica: Experimental and modeling investigations", *Case Studies in Construction Materials*, 16, e01036, <https://doi.org/10.1016/j.cscm.2022.e01036>.
- Ahmed, H.U., Mohammed, A.S. and Mohammed, A.A. (2022). "Proposing several model techniques including ANN and M5P-tree to predict the compressive strength of geopolymer concretes incorporated with nano-silica", *Environmental Science and Pollution Research*, 29(47), 71232-71256. <https://doi.org/10.1007/s11356-022-20863-1>.
- Alberti, M.G., Enfedaque, A. and Gálvez, J.C. (2015). "Improving the reinforcement of polyolefin fiber reinforced concrete for infrastructure applications", *Fibers*, 3(4), 504-522, <https://doi.org/10.3390/fib3040504>.
- Albitar, M., Ali, M.M., Visintin, P. and Drechsler, M. (2017). "Durability evaluation of geopolymer and conventional concretes", *Construction and Building Materials*, 136, 374-385, <https://doi.org/10.1016/j.conbuildmat.2017.01.056>.
- Albidah, A., Alqarni, A.S., Abbas, H., Almusallam, T. and Al-Salloum, Y. (2022). "Behavior of Metakaolin-Based geopolymer concrete at ambient and elevated temperatures", *Construction and Building Materials*, 317, 125910, <https://doi.org/10.1016/j.conbuildmat.2021.125910>.
- Amin, M., Elsakhawy, Y., Abu el-hassan, K. and Abdelsalam, B.A. (2022). "Behavior evaluation of sustainable high strength geopolymer concrete based on fly ash, metakaolin, and slag", *Case Studies in Construction Materials*, 16, e00976, <https://doi.org/10.1016/j.cscm.2022.e00976>.
- Amran, M., Huang, S.S., Debbarma, S. and Rashid, R.S. (2022). "Fire resistance of geopolymer concrete: A critical review", *Construction and Building Materials*, 324, 126722, <https://doi.org/10.1016/j.conbuildmat.2022.126722>.
- Asadi, I., Baghban, M.H., Hashemi, M., Izadyar, N. and Sajadi, B. (2022). "Phase change materials incorporated into geopolymer concrete for enhancing energy efficiency and sustainability of buildings: A review", *Case Studies in Construction Materials*, 17, e01162, <https://doi.org/10.1016/j.cscm.2022.e01162>.
- Assaedi, H., Alomayri, T., Shaikh, F. and Low, I.M. (2019). "Influence of nano silica particles on durability of flax fabric reinforced geopolymer composites" *Materials*, 12(9), 1459, <https://doi.org/10.3390/ma12091459>.
- Aslani, F. (2016). "Thermal performance modeling of geopolymer concrete", *Journal of Materials in Civil Engineering*, 28(1), 04015062, [https://doi.org/10.1061/\(ASCE\)MT.1943-5533.000129](https://doi.org/10.1061/(ASCE)MT.1943-5533.000129).
- Bentz, D.P. (2000). "Fibers, percolation, and spalling of high-performance concrete", *Materials Journal*, 97(3), 351-359, <https://www.researchgate.net/publication/234155149>.
- Connolly, D.P., Kouroussis, G., Woodward, P.K., Giannopoulos, A., Verlinden, O. and Forde, M. C. (2014). "Scoping prediction of re-radiated ground-borne noise and vibration near high speed rail lines with variable soils", *Soil Dynamics and Earthquake Engineering*, 66, 78-88, <https://doi.org/10.1016/j.soildyn.2014.06.021>.
- Deb, P.S., Sarker, P.K. and Barbhuiya, S. (2016). "Sorptivity and acid resistance of ambient-cured geopolymer mortars containing nano-silica", *Cement and Concrete Composites*, 72, 235-245, <https://doi.org/10.1016/j.cemconcomp.2016.06.017>.
- De Beer, F.C., Le Roux, J.J. and Kearsley, E.P. (2005). "Testing the durability of concrete with neutron radiography", *Nuclear Instruments and Methods in Physics Research Section A: Accelerators, Spectrometers, Detectors and Associated Equipment*, 542(1-3), 226-231, <https://doi.org/10.1016/j.nima.2005.01.104>.
- Du, H., Du, S. and Liu, X. (2014). "Durability performances of concrete with nano-silica", *Construction and Building Materials*, 73, 705-712, <https://doi.org/10.1016/j.conbuildmat.2014.10.014>.
- Erfanimanesh, A. and Sharbatdar, M.K. (2020). "Mechanical and microstructural characteristics of geopolymer paste, mortar, and concrete containing local zeolite and slag activated by sodium carbonate", *Journal of Building Engineering*, 32, 101781, <https://doi.org/10.1016/j.jobe.2020.101781>.
- Fan, F., Liu, Z., Xu, G., Peng, H. and Cai, C.S. (2018). "Mechanical and thermal properties of fly ash based geopolymers", *Construction and Building Materials*, 160, 66-81, <https://doi.org/10.1016/j.conbuildmat.2017.11.023>.
- Fallah Hosseini, S. and Hajikarimi, P. (2019). "Investigation on the effect of volume, length and shape of Polyolefin Fibers on mechanical characteristics and fracture properties of high-strength concrete", *Concrete Research*, 12(1), 59-70, [https://jcr.guilan.ac.ir/article\\_3176.html](https://jcr.guilan.ac.ir/article_3176.html).
- Galan, A. (1967). "Estimate of concrete strength by ultrasonic pulse velocity and damping constant", *Journal Proceedings*, 64(10), 678-684.

- Hu, S.G., Wu, J., Yang, W., He, Y.J., Wang, F.Z. and Ding, Q.J. (2009). "Preparation and properties of geopolymer-lightweight aggregate refractory concrete", *Journal of Central South University of Technology*, 16(6), 914-918, <https://link.springer.com/article/10.1007/s11771-009-0152-x>.
- Jindal, B.B., Alomayri, T., Hasan, A. and Kaze, C. R. (2022). "Geopolymer concrete with metakaolin for sustainability: A comprehensive review on raw material's properties, synthesis, performance, and potential application", *Environmental Science and Pollution Research*, 30, 25299-25324, <https://doi.org/10.1007/s11356-021-17849-w>.
- Kanagaraj, B., Anand, N., Alengaram, U.J., Raj, R. S. and Kiran, T. (2022). "Exemplification of sustainable sodium silicate waste sediments as coarse aggregates in the performance evaluation of geopolymer concrete", *Construction and Building Materials*, 330, 127135, <https://doi.org/10.1016/j.conbuildmat.2022.127135>.
- Kwan, W.H., Ramli, M., Kam, K.J. and Sulieman, M.Z. (2012). "Influence of the amount of recycled coarse aggregate in concrete design and durability properties" *Construction and Building Materials*, 26(1), 565-573, <https://doi.org/10.1016/j.conbuildmat.2011.06.059>.
- Law, D.W., Adam, A.A., Molyneaux, T.K., Patnaikuni, I. and Wardhono, A. (2015). "Long term durability properties of class F fly ash geopolymer concrete", *Materials and Structures*, 48(3), 721-731, <https://doi.org/10.1617/s11527-014-0268-9>.
- Lyu, X., Robinson, N., Elchalakani, M., Johns, M. L., Dong, M. and Nie, S. (2022). "Sea sand seawater geopolymer concrete", *Journal of Building Engineering*, 50, 104141, <https://doi.org/10.1016/j.jobe.2022.104141>.
- Mansourghanaei, M., Biklaryan, M., and Mardookhpour, A. (2022). "Experimental study of the effects of adding silica nanoparticles on the durability of geopolymer concrete", *Australian Journal of Civil Engineering*, 1-13, <https://doi.org/10.1080/14488353.2022.2120247>.
- Memiş, S. and Bilal, M.A.M. (2022). "Taguchi optimization of geopolymer concrete produced with rice husk ash and ceramic dust", *Environmental Science and Pollution Research*, 29(11), 15876-15895, <https://doi.org/10.1007/s11356-021-16869-w>.
- Mansourghanaei, M. (2022). "Experimental evaluation of compressive, tensile strength and impact test in blast furnace slag based geopolymer concrete, under high temperature", *Journal of Civil Engineering Researchers*, 4(2), 12-21, <https://doi.org/10.52547/JCER.4.2.12>.
- Mansourghanaei, M. (2022). "Experimental study of compressive strength, permeability and impact testing in geopolymer concrete based on Blast furnace slag", *Journal of Civil Engineering Researchers*, 4(3), 31-39, <https://doi.org/10.52547/JCER.4.3.31>.
- Morsy, M.S., Al-Salloum, Y.A., Abbas, H. and Alsayed, S.H. (2012). "Behavior of blended cement mortars containing nano-metakaolin at elevated temperatures", *Construction and Building Materials*, 35, 900-905, <https://doi.org/10.1016/j.conbuildmat.2012.04.099>.
- Mustakim, S.M., Das, S.K., Mishra, J., Aftab, A., Alomayri, T.S., Assaedi, H.S. and Kaze, C.R. (2021). "Improvement in fresh, mechanical and microstructural properties of fly ash-GBFS based geopolymer concrete by addition of nano and micro silica", *Silicon*, 13(8), 2415-2428, <https://doi.org/10.1007/s12633-020-00593-0>.
- Nazari, A. and Sanjayan, J.G. (2015). "Hybrid effects of alumina and silica nanoparticles on water absorption of geopolymers: Application of Taguchi approach", *Measurement*, 60, 240-246, <https://doi.org/10.1016/j.measurement.2014.10.004>.
- Phoo-ngernkham, T., Chindaprasirt, P., Sata, V., Hanjitsuwan, S. and Hatanaka, S. (2014). "The effect of adding nano-SiO<sub>2</sub> and nano-Al<sub>2</sub>O<sub>3</sub> on properties of high calcium fly ash geopolymer cured at ambient temperature", *Materials and Design*, 55, 58-65, <https://doi.org/10.1016/j.matdes.2013.09.049>.
- Phair, J. W. and Van Deventer, J.S.J. (2002). "Effect of the silicate activator pH on the microstructural characteristics of waste-based geopolymers", *International Journal of Mineral Processing*, 66(1-4), 121-143, [https://doi.org/10.1016/S0301-7516\(02\)00013-3](https://doi.org/10.1016/S0301-7516(02)00013-3).
- Rashad, A.M. and Zeedan, S.R. (2012). "A preliminary study of blended pastes of cement and quartz powder under the effect of elevated temperature", *Construction and Building Materials*, 29, 672-681, <https://doi.org/10.1016/j.conbuildmat.2011.10.006>.
- Rendell, F., Jauberthie, R. and Grantham, M. (2002). *Deteriorated concrete: Inspection and physicochemical analysis*, Thomas Telford.
- Ren, W., Xu, J. and Bai, E. (2016). "Strength and ultrasonic characteristics of alkali-activated fly ash-slag geopolymer concrete after exposure to elevated temperatures", *Journal of Materials in Civil Engineering*, 28(2), 04015124, [https://doi.org/10.1061/\(ASCE\)MT.1943-5533.000140](https://doi.org/10.1061/(ASCE)MT.1943-5533.000140).
- Reufi, E., Marku, J. and Bier, T. (2016). "Ultrasonic pulse velocity investigation of Polypropylene

- and steel fiber reinforced concrete”, *International Journal of Civil and Environmental Engineering*, 10(3), 332-335, <https://doi.org/10.5281/zenodo.1112125>.
- Sathish Kumar, V., Ganesan, N., Indira, P.V., Murali, G. and Vatin, N.I. (2022). “Flexural behaviour of hybrid fibre-reinforced ternary blend geopolymer concrete beams”, *Sustainability*, 14(10), 5954, <https://doi.org/10.3390/su14105954>.
- Shilar, F.A., Ganachari, S.V., Patil, V.B., Khan, T. Y. and Dawood, S. (2022). “Molarity activity effect on mechanical and microstructure properties of geopolymer concrete: A review”, *Case Studies in Construction Materials*, 16, e01014, <https://doi.org/10.1016/j.cscm.2022.e01014>.
- Shilar, F.A., Ganachari, S.V., Patil, V.B., Khan, T. Y., Almakayeel, N.M. and Alghamdi, S. (2022). “Review on the relationship between nano modifications of geopolymer concrete and their structural characteristics”, *Polymers*, 14(7), 1421, <https://doi.org/10.3390/polym14071421>.
- Srividya, T., PR, K.R., Sivasakthi, M., Sujitha, A., and Jeyalakshmi, R. (2022). “A state-of-the-art on development of geopolymer concrete and its field applications”, *Case Studies in Construction Materials*, 16, e00812, <https://doi.org/10.1016/j.cscm.2021.e00812>.
- Türkmen, İ., Karakoç, M B., Kantarcı, F., Maraş, M.M. and Demirboğa, R. (2016). “Fire resistance of geopolymer concrete produced from Elazığ ferrochrome slag”, *Fire and Mmaterials*, 40(6), 836-847, <https://doi.org/10.1002/fam.2348>.
- Verma, M. and Dev, N. (2022). “Effect of liquid to binder ratio and curing temperature on the engineering properties of the geopolymer concrete” *Silicon*, 14(4), 1743-1757, <https://doi.org/10.1007/s12633-021-00985-w>.
- Verma, M., Dev, N., Rahman, I., Nigam, M., Ahmed, M. and Mallick, J. (2022). “Geopolymer concrete: A material for sustainable development in Indian construction industries”, *Crystals*, 12(4), 514, <https://doi.org/10.3390/cryst12040514>.
- Whitehurst, E.A. (1951). “Sonoscope tests concrete structures”, *Journal Proceedings*, 47(2), 433-444.
- Wong, L.S. (2022). “Durability performance of geopolymer concrete: A review”, *Polymers*, 14(5), 868, <https://doi.org/10.3390/polym14050868>.
- Yousefvand, M., Sharifi, Y. and Yousefvand, S. (2019). “An analysis of the shear strength and rupture modulus of Polyolefin-Fiber reinforced concrete at different temperatures”, *Journal of Civil Engineering and Materials Application*, 3(4), 225-233, <https://doi.org/10.3390/polym14050868>.



This article is an open-access article distributed under the terms and conditions of the Creative Commons Attribution (CC-BY) license.